Promega

GloMax®
Microplate Readers

A better way to detect luminescence.

Accurate results from every well

•

Sensitive Detection

•

Low Crosstalk

Learn more about GloMax ››

STEM CELLS®

TISSUE-SPECIFIC STEM CELLS

c-Met Signaling Is Essential for Mouse Adult Liver Progenitor Cells Expansion After Transforming Growth Factor-β-Induced Epithelial–Mesenchymal Transition and Regulates Cell Phenotypic Switch

LAURA ALMALÉ,[a] MARÍA GARCÍA-ÁLVARO,[a] ADORACIÓN MARTÍNEZ-PALACIÁN,[a] MARÍA GARCÍA-BRAVO,[b,c,d] NEREA LAZCANOITURBURU,[a] ANNALISA ADDANTE,[a] CESÁREO RONCERO,[a] JULIÁN SANZ,[e] MARÍA DE LA O LÓPEZ,[a] PALOMA BRAGADO,[a] WOLFGANG MIKULITS,[f] VALENTINA M. FACTOR,[g] SNORRI S. THORGEIRSSON,[g,h] J. IGNACIO CASAL,[i] JOSÉ-CARLOS SEGOVIA,[b,c,d] EDUARDO RIAL,[j] ISABEL FABREGAT,[k,l] BLANCA HERRERA,[a,†] ARÁNZAZU SÁNCHEZ [a,†]

Key Words. HGF/c-Met • Oval cell • TGF-β • EMT

ABSTRACT

Adult hepatic progenitor cells (HPCs)/oval cells are bipotential progenitors that participate in liver repair responses upon chronic injury. Recent findings highlight HPCs plasticity and importance of the HPCs niche signals to determine their fate during the regenerative process, favoring either fibrogenesis or damage resolution. Transforming growth factor-β (TGF-β) and hepatocyte growth factor (HGF) are among the key signals involved in liver regeneration and as component of HPCs niche regulates HPCs biology. Here, we characterize the TGF-β-triggered epithelial–mesenchymal transition (EMT) response in oval cells, its effects on cell fate in vivo, and the regulatory effect of the HGF/c-Met signaling. Our data show that chronic treatment with TGF-β triggers a partial EMT in oval cells based on coexpression of epithelial and mesenchymal markers. The phenotypic and functional profiling indicates that TGF-β-induced EMT is not associated with stemness but rather represents a step forward along hepatic lineage. This phenotypic transition confers advantageous traits to HPCs including survival, migratory/invasive and metabolic benefit, overall enhancing the regenerative potential of oval cells upon transplantation into a carbon tetrachloride-damaged liver. We further uncover a key contribution of the HGF/c-Met pathway to modulate the TGF-β-mediated EMT response. It allows oval cells expansion after EMT by controlling oxidative stress and apoptosis, likely via Twist regulation, and it counterbalances EMT by maintaining epithelial properties. Our work provides evidence that a coordinated and balanced action of TGF-β and HGF are critical for achievement of the optimal regenerative potential of HPCs, opening new therapeutic perspectives. STEM CELLS *2019;37:1108–1118*

SIGNIFICANCE STATEMENT

The findings from this study support that a balanced action of transforming growth factor-β and hepatocyte growth factor could determine liver progenitor's fate and the outcome of liver regeneration, and open possibilities for targeted therapies oriented at improving the regenerative capacity of these cells in chronic liver diseases.

INTRODUCTION

Adult hepatic progenitor cells (HPCs), known in rodent as oval cells, expand in situations of chronic liver damage or diseases in which hepatocyte proliferation and function are impaired and thus becoming a critical asset to orchestrate liver repair response [1, 2]. The progenitor-associated liver regeneration and supporting signals are still not well characterized. A good understanding of the regulation of HPCs is crucial not only because their regenerative potential makes them interesting therapeutic targets in liver pathologies, but also because increasing evidence points to a role of oval cells in progression of liver fibrosis [3, 4], leaving the question on the role of oval cells in the context of chronic liver disease (CLD) open.

Transforming growth factor-β (TGF-β) is a central regulator in CLD contributing to seemingly all stages of disease [5, 6]. Once TGF-β is activated upon damage, it triggers crucial cellular events that drive disease progression. Thus, it promotes hepatic stellate cell (HSC) transdifferentiation into myofibroblast, the main

[a]Department of Biochemistry and Molecular Biology, Faculty of Pharmacy, Complutense University of Madrid, Health Research Institute of the Hospital Clínico San Carlos, Madrid, Spain; [b]Cell Differentiation and Cytometry Unit, Hematopoietic Innovative Therapies Division, Centro de Investigaciones Energéticas, Medioambientales y Tecnológicas (CIEMAT), Madrid, Spain; [c]Centro de Investigación Biomédica en Red de Enfermedades Raras (CIBERER), Madrid, Spain; [d]Advanced Therapies Mixed Unit, CIEMAT/IIS Fundación Jiménez Díaz, Madrid, Spain; [e]Department of Pathology, Hospital Clínico San Carlos, Madrid, Spain; [f]Department of Medicine I, Institute of Cancer Research, Comprehensive Cancer Center, Medical University of Vienna, Vienna, Austria; [g]Laboratory of Experimental Carcinogenesis, National Cancer Institute, National Institutes of Health, Bethesda, Maryland, USA; [h]Laboratory of Human Carcinogenesis, Center for Cancer Research, National Cancer Institute, National Institutes of Health, Bethesda, Maryland; [i]Department of Functional Proteomics, Centro de Investigaciones Biológicas (CIB-CSIC), Madrid, Spain; [j]Department of Cellular and Molecular Medicine, Centro de Investigaciones Biológicas (CIB-CSIC), Madrid, Spain; [k]TGF-β and Cancer Group, Oncobell Program, Bellvitge Biomedical Research Institute (IDIBELL) and University of Barcelona, L'Hospitalet de Llobregat, Barcelona, Spain; [l]Oncology Program, CIBEREHD, National Biomedical Research Institute on Liver and Gastrointestinal Diseases, Instituto de Salud Carlos III, Madrid, Spain

Correspondence: Aránzazu Sánchez, Ph.D., Department of Biochemistry and Molecular Biology, Faculty of Pharmacy, Complutense University of Madrid, Plaza Ramón y Cajal S/N, 28040 Madrid, Spain. Telephone: 34913941855; e-mail: munozas@ucm.es

Received October 23, 2018; accepted for publication April 29, 2019; first published online May 20, 2019.

http://dx.doi.org/10.1002/stem.3038

[†]Co-senior authors.

The data that support the findings of this study are available from the corresponding author upon reasonable request.

source of extracellular matrix (ECM) during liver fibrosis and the main producer of TGF-β [7]. TGF-β also targets other cell types that contribute to the progression of CLD. Indeed, both oxidative stress and apoptosis of hepatocytes are well-established hallmarks of the fibrotic process [8], both modulated by TGF-β [9, 10]. Reactive oxygen species (ROS) and TGF-β are interconnected by feedforward and feedback loops [11], and evidence supports that hepatocyte loss contributes to hepatic fibrosis by directly inducing HSC activation [8, 12]. Additionally, TGF-β is well known as a potent inducer of epithelial–mesenchymal transition (EMT) in different cell types, including hepatocytes [13, 14]. This phenotypic transition is orchestrated by a set of specific transcription factors (TFs) called EMT-inducing TFs (Snail, Zeb1, Zeb2, and others) that are responsible for the changes in gene expression ultimately leading to the loss of epithelial markers (e.g., E-cadherin) and acquisition of mesenchymal markers (e.g., N-cadherin and vimentin) [15]. The possibility that EMT contributes to hepatic fibrogenesis in CLD is an issue not exempt of controversy [16–19]. Nevertheless, it reinforces the idea that other liver cells, apart from the HSC, may play a role during liver fibrosis. Whether HPCs are targets for the profibrotic effects of TGF-β in CLD remain unclear. In this sense, evidence of TGF-β-induced EMT in HPCs exists [20, 21] but the regulation of this response, the consequences for cell fate, or the outcome of the repair response remain obscure.

As opposed to TGF-β, hepatocyte growth factor (HGF)/c-Met signaling has a hepatoprotective effect attenuating liver fibrosis. HGF/c-Met mediates survival of hepatocytes [22] while inducing apoptosis in activated HSCs and promoting ECM resolution [23, 24]. The antifibrotic action of HGF has been associated with both inhibition of TGF-β expression and counteraction of TGF-β profibrotic activities, particularly repressing TGF-β-stimulated profibrogenic gene transcription and EMT [25–28]. These and other findings provide a picture where TGF-β and HGF/c-Met play opposite and key roles in liver injury and repair modulating each other responses, creating a functional network that operates in diseased liver. Generation of c-Met and HGF mutant mice has allowed to prove the remarkable and unique proregenerative capacity of HGF/c-Met signaling both in acute as well as chronic liver injuries involving both hepatocytes and HPCs [29–31]. In the past, we have also provided evidence supporting a functional interaction between TGF-β and c-Met signaling in oval cells in vitro that fine-tunes the cell responses, specifically the TGF-β-driven oxidative stress and cell death [32, 33]. However, whether a crosstalk between these two signaling pathways can modulate other responses in HPCs during chronic liver injury and how it could affect the outcome of the regenerative response is not known. In this work, we aimed to characterize the response of oval cells to chronic treatment with TGF-β to emulate the situation of a chronic liver damage. We also addressed the role of the HGF/c-Met signaling axis on the regulation of this response.

Materials and Methods

Cell Lines and Culture Conditions

$Met^{flx/flx}$ and $Met^{-/-}$ oval cell lines were generated and maintained as described [32]. To generate chronically TGF-β-treated cells (TβT-OC), oval cells were treated for 2 days with TGF-β (1 ng/ml). Thereafter, the remaining cells were cultured in medium supplemented with 10% fetal bovine serum and TGF-β (0.5 ng/ml) and subcultured when they reached confluence. For further passages, medium was always supplemented with 0.5 ng/ml of TGF-β. Cells were submitted to subsequent passages to establish a stable cell line of TβT-OC. At least three different TβT-OC lines were used for phenotypic and functional studies. Ras-oval cells were generated by lentiviral transduction of $Met^{flx/flx}$ oval cells with oncogenic v-Ha-Ras followed by selection of green fluorescent protein (GFP) positive cells by fluorescence-activated cell sorting. For transplantation experiments, GFP expressing oval cells (parental $Met^{flx/flx}$ oval cells and TβT-OC) were generated by lentiviral transduction of oval cells with the lentiviral vector pLVX-SFFV-zsGFP (generated at CIEMAT) modified from pLVX-IRES-ZsGreen1 Vector (Clontech) followed by selection of GFP-positive cells by fluorescence-activated cell sorting.

RNA Isolation, Quantitative, and Semiquantitative Reverse Transcriptase-Polymerase Chain Reaction

Total cellular RNA was isolated using the RNeasy Kit (Qiagen, Valencia, CA). RNA yield and purity were analyzed using a spectrophotometer (ultraviolet–visible recording spectrophotometer Specord 205, AnalytikJena, Jena, Germany). Quantitative reverse transcriptase-polymerase chain reaction (RT-qPCR) and RT-PCR were performed as described before [32, 33]. Primers used in the study are listed in Supporting Information Table S1.

Measurement of Intracellular ROS

For the analysis of intracellular ROS, the oxidation-sensitive probe 2′,7′-dichlorodihydrofluorescein diacetate (DCFH-DA) (5 μM) was used as described [10]. For flow cytometry analysis, cells were detached by trypsinization and cellular fluorescence intensity was measured after 30 minutes incubation with DCFH-DA, by using FACSCalibur flow cytometer. Ten thousand cells were recorded in each analysis. For confocal microscopy analysis, cells were washed twice with phosphate-buffered saline (PBS) and incubated for 30 minutes with DCFH-DA. The fluorescence intensity was analyzed using an OLYMPUS FV1200 fluorescence microscope. Photographs were taken with ×60 objective.

Carbon Tetrachloride-Induced Liver Fibrosis Model for Cell Transplantation

C57BL/6JOlaHsd mice were housed in the Complutense University of Madrid (UCM) animal facility in temperature-controlled rooms under a 12-hour light/dark cycle and allowed food and water ad libitum. Mice were routinely screened for pathogens in accordance with Federation of European Laboratory Animal Science Associations procedures. Experimental procedures were approved by the Institutional and Regional Committee for Animal Care and Use (PROEX 305/15).

To induce liver damage, we followed a protocol described by Awan et al. [34]. Five- to nine-week-old mice received biweekly intraperitoneal injections of 3 μl/g carbon tetrachloride (CCl_4; 10% in mineral oil) before transplantation (for 4 weeks) and after transplantation (for 1 or 8 weeks). At transplantation, mice were randomly divided into PBS-group (animals injected with PBS); animals transplanted with OC-GFP and animals transplanted with TβT-OC-GFP. $Met^{flx/flx}$ oval cell lines carrying the floxed allele were used in both cases (OC-GFP, TβT-OC-GFP) to allow cell tracking in livers upon injection. Transplantation was performed as follows: spleen was exposed by a left flank incision, where PBS (100 μl) or cells (2.5×10^6/100 μl PBS) were slowly infused with a gauge needle. Homeostasis was achieved by ligation of the splenic tip. Animals belonging

to the different groups were sacrificed 1 week or 8 weeks after transplantation.

Statistical Analysis

Mean ± SEM were used to describe each of the variables analyzed. An unpaired Student's *t* test or one-way analysis of variance followed by the Bonferroni post hoc test were used to compare different variables between two or more experimental groups, respectively. Longitudinal studies were performed using paired or unpaired Student's *t* test as appropriate. For all analysis, *p* values below .05 were considered statistically significant and were indicated in each figure. All statistical analyses were performed using GraphPad Prism 8 software (San Diego, CA). For more details and other methods, see Supporting Information.

Results

TGF-β-Induced EMT in Oval Cells Is Associated with Profound Alterations in Hepatic Lineage Markers and Decreased Stemness

To analyze the TGF-β-triggered EMT response in oval cells, we treated $Met^{flx/flx}$ oval cell lines with TGF-β both acutely (1 ng/ml TGF-β, 48 hours) and chronically (1 ng/ml TGF-β 48 hours followed by continuous subculture in the presence of 0.5 ng/ml of TGF-β). Cells chronically exposed to TGF-β are referred herein to as TGF-β-treated oval cells (TβT-OC) to distinguish them from parental untreated oval cells. Activation of the TGF-β pathway in both oval cells acutely treated with TGF-β and TβT-OC was demonstrated by induction of early TGF-β downstream targets (Smad7, Pai1, Ski1; Supporting Information Fig. S1). We confirmed that Snail (*Snai1*), one of the most relevant EMT-inducing TF was upregulated in all oval cell lines treated with TGF-β (Fig. 1A). Furthermore, mesenchymal markers such as N-cadherin and vimentin were upregulated in TβT-OC (Fig. 1B). E-cadherin expression, a cell–cell contact protein characteristic of epithelial cells, showed a clear downregulation upon acute treatment with TGF-β. However, chronically treated cells showed heterogeneous E-cadherin expression, with some TβT-OC lines expressing low and others high E-cadherin levels (Fig. 1), suggesting a partial rather than a full EMT. Nevertheless, an overall mesenchymal cell phenotype of TβT-OC was consistent with a decreased expression of cadherin-17, a member of the cadherin family expressed exclusively in epithelial cells of the gastrointestinal system [35], and a strong downregulation of occludin, a protein component of tight junctions (Fig. 1B). Additionally, the subcellular localization pattern of the tight junction protein zonula occludens-1 (ZO-1) changed from cell to cell contact sites to a diffuse intracellular distribution (Fig. 1C), a common phenomenon during EMT [36]. These molecular changes were associated with a switch toward a mesenchymal-like morphology, overall demonstrating a phenotypic transition consistent with an EMT. Interestingly, phenotypic transition appears to become irreversible since removal of TGF-β does not result in decrease of mesenchymal markers like vimentin despite Snail downregulation (Supporting Information Fig. S2).

Typically, the EMT process induced by TGF-β in epithelial cells correlates with a less differentiated phenotype and acquisition of stem cell properties [37]. To analyze if the TGF-β-induced EMT could affect oval cell lineage properties and/or stemness, we checked the expression of stem cell markers Epcam, CD133, CD44, and CD90 by flow cytometry, Western blot, and/or RT-qPCR (Fig. 2A, 2B and Supporting Information Fig. S3). In TβT-OC, there was a downregulation of Epcam and CD133, markers usually associated with epithelial cells [38], whereas the expression of the mesenchymal-related marker CD44 was not altered and CD90 expression increased. Additionally, TβT-OC did not show an advantage neither on clonal growth capacity, which actually decreased, or spheroids-forming ability under anchorage-independent conditions (Fig. 2C, 2D). These results suggest that EMT induced in oval cells by chronic treatment with TGF-β does not result in acquisition of stem cell properties. Since Epcam is also used as a marker of HPCs [1, 39], and its expression was decreased in TβT-OC, we further explored the EMT effects on the intrinsic lineage features of oval cells, which are bipotential progenitor cells that can differentiate into hepatocytes or cholangiocytes. Expression of CK19 and albumin, additional common markers of oval cells, did not change or slightly increased (albumin; Fig. 2E, 2F). However, γ-glutamyltransferase (GGT) and HNF1β, biliary epithelial markers that are expressed in oval cells and hepatoblasts but downregulated during hepatocyte maturation, showed a sharp decrease. Furthermore, alpha-fetoprotein (AFP), a hepatocyte-specific gene for an early process of hepatocyte differentiation, and HNF4α, a transcription factor known to drive hepatocyte differentiation [40] were upregulated (Fig. 2G). Altogether, data suggest a switch to a more mature hepatic phenotype in TβT-OC, phenotype that also persists after TGF-β removal (Supporting Information Fig. S2).

EMT Confers Functional Advantages to Oval Cells, Which Enhance Their Regenerating Capacity

EMT confers cells a series of advantages, including increased proliferation, migratory/invasive capacities, and resistance to apoptosis among others [41, 42]. TβT-OC showed identical cell growth rate in the presence of serum as compared with parental cells (Fig. 3A). Although serum withdrawal induces apoptosis in oval cells [32], TβT-OC maintained an intrinsic growth capacity in the absence of serum (Fig. 3B). Furthermore, cells chronically treated with TGF-β no longer responded to TGF-β with apoptotic cell death (Fig. 3C, 3D) and increase in ROS production (Supporting Information Fig. S4A), the latter being an event critical for TGF-β-induced apoptosis [33] that involves the activity of NADPH oxidases, particularly Nox4 (Supporting Information Fig. S4B, S4C). In addition, TβT-OC acquired a higher migratory and invasive phenotype, as evidenced by transwell invasion assays, and increased activity of ECM-degrading metalloproteinases (Fig. 3E and Supporting Information S5A, S5B). TβT-OC also switched the bioenergetic profile toward a more glycolytic phenotype when compared with the normal counterparts as revealed by a lower ratio of respiration to glycolysis, determined by the extracellular acidification rate, and confirmed by increased lactate production (Fig. 3F, 3G). Noteworthy, TβT-OC metabolic profile was similar to that of oval cells transformed with oncogenic Ras (Ras-OC), used as a comparative reference for tumorigenic cells. However, TGF-β-OC did not acquire anchorage independent growth capacity (Fig. 3H), indicating that TGF-β-induced EMT confers selective functional advantages but does not drive malignant transformation.

In a next step, we analyzed whether the profound changes observed in TβT-OC conferred cell growth/survival advantages in vivo, in the context of injured liver. To this end, we performed intrasplenic injection of parental oval cells and TβT-OC transduced with GFP in mice subjected to a chemically induced liver fibrosis (Fig. 4A). Engraftment of parental and TβT-OC

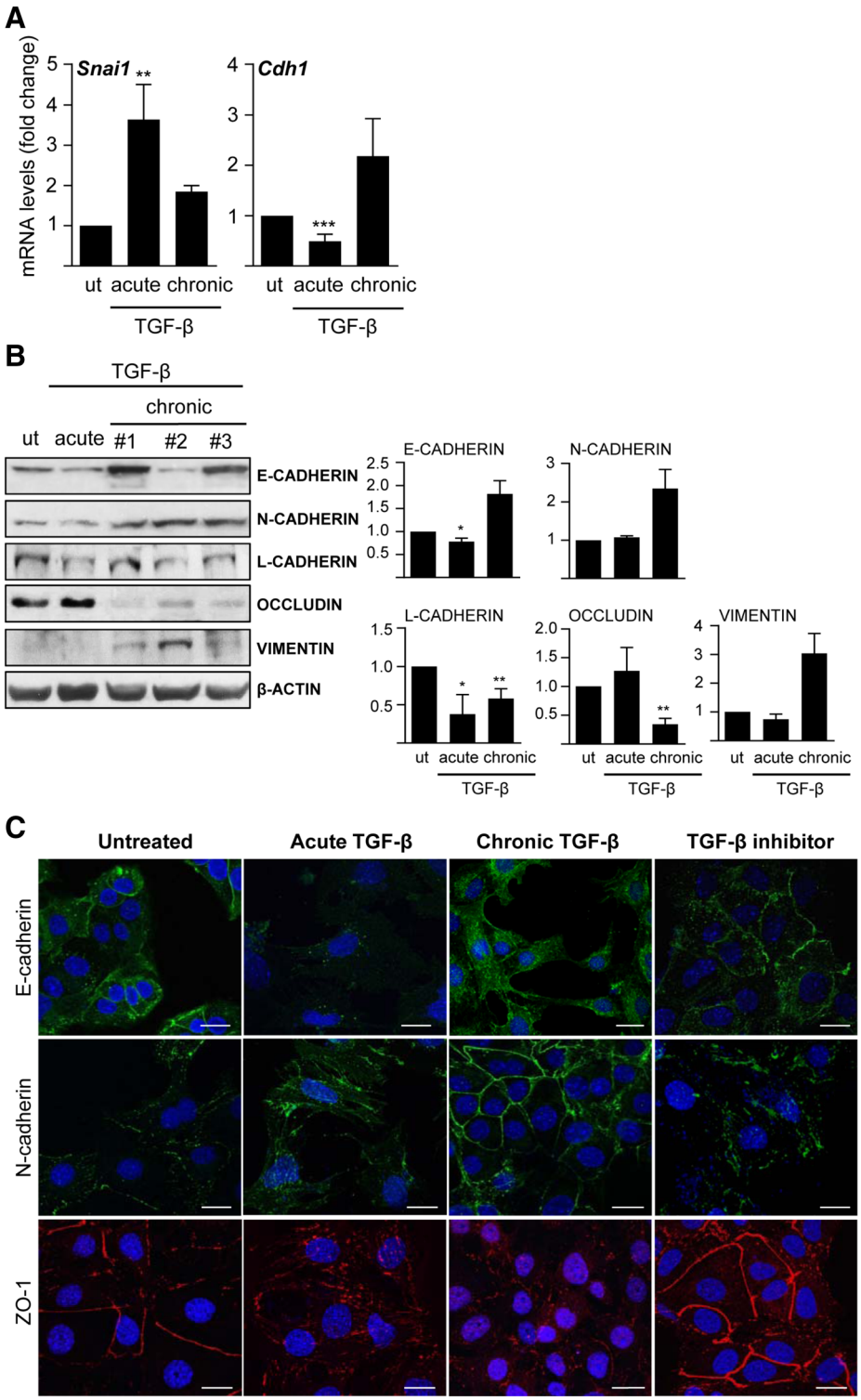

Figure 1. Epithelial and mesenchymal markers in oval cells treated or not with transforming growth factor-β (TGF-β). **(A):** *Snai* and *Cdh1* mRNA levels in oval cells acutely or chronically treated with TGF-β were determined by quantitative reverse transcriptase-polymerase chain reaction. Data are mean ± SEM of 11 experiments. **(B):** Oval cells were acutely or chronically treated with TGF-β and protein lysates were collected to perform a Western blot analysis. β-Actin was used as a loading control. One representative experiment using three different TβT-OC (designated #1, #2, and #3) is shown (left panel). Optical density values are mean ± SEM of 3–5 independent experiments (n = 3–18; right panel). **(C):** Confocal microscopy images of oval cells untreated and chronically treated with TGF-β oval cells. Cells acutely treated with TGF-β in the absence or presence of 10 μm SB431542 (TGF-β inhibitor) were also included as positive or negative controls of TGF-β response. Representative images out of 2–3 experiments are shown. Scale bar: 20 μm. In all cases, data were compared with the untreated group; *, $p < .05$; **, $p < .01$. At least three different TβT-OC lines were used in all analyses.

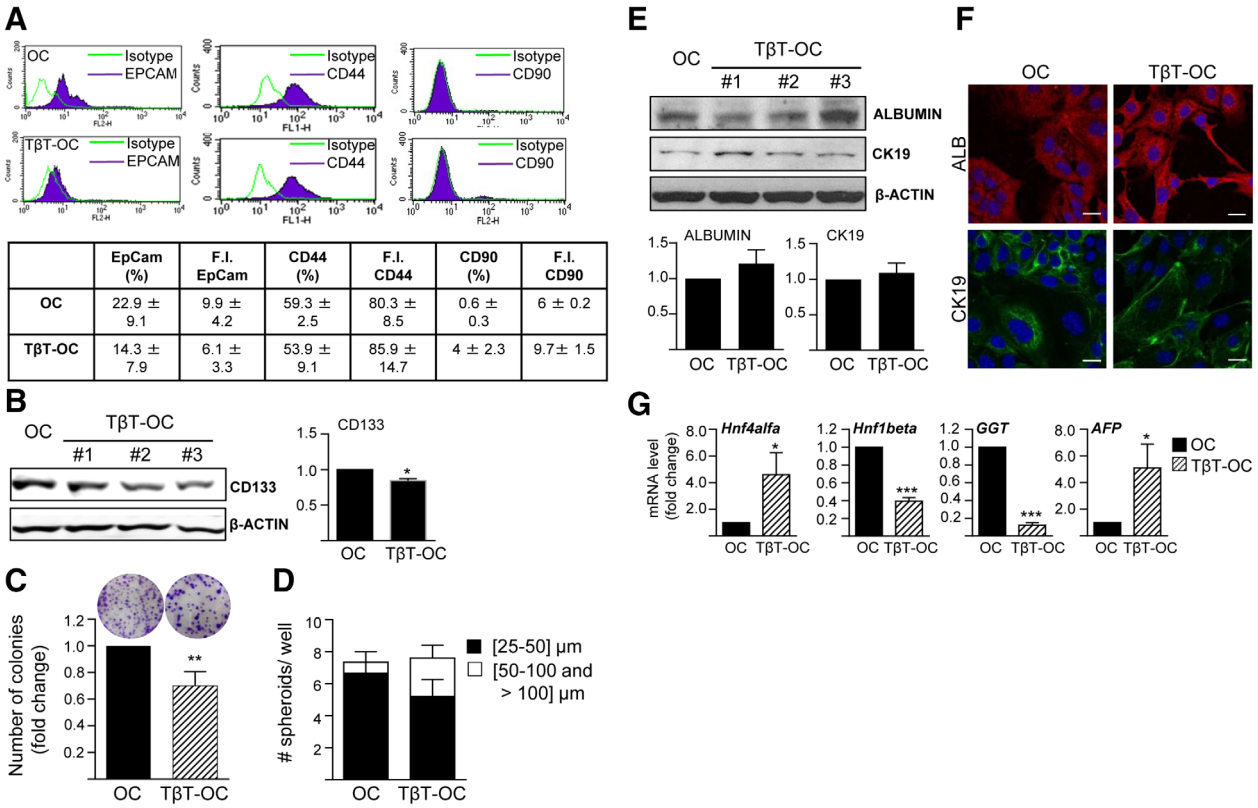

	EpCam (%)	F.I. EpCam	CD44 (%)	F.I. CD44	CD90 (%)	F.I. CD90
OC	22.9 ± 9.1	9.9 ± 4.2	59.3 ± 2.5	80.3 ± 8.5	0.6 ± 0.3	6 ± 0.2
TβT-OC	14.3 ± 7.9	6.1 ± 3.3	53.9 ± 9.1	85.9 ± 14.7	4 ± 2.3	9.7± 1.5

Figure 2. Hepatic lineage markers and stemness in oval cells before and after chronic treatment with transforming growth factor-β. **(A):** Epcam, CD44, and CD90 expressions in oval cells and TβT-OC were analyzed by flow cytometry. A representative experiment is shown (upper panel). Percentage of positive cells and fluorescence intensity values are mean ± SEM of two independent experiments (n = 2–6; lower panel). **(B):** CD133 protein levels in oval cells and TβT-OC by Western blot. β-Actin used as a loading control. One representative experiment using three different TβT-OC (designated #1, #2, and #3) is shown (left panel). Optical density values are mean ± SD of one experiment (n = 2–3; right panel). **(C):** Clonogenic assay in oval cells and TβT-OC. Graph represents number of clones. Data are mean ± SEM of three independent experiments (n = 6–8). Representative images are included. **(D):** The number of spheroids in the absence of attachment per well is shown, distributed according to their diameter. Data are mean ± SEM of two independent experiments (n = 2–5). **(E):** Albumin and ck19 protein by Western blot in the same conditions as in (B), one representative experiment (upper panel). Optical density values are mean ± SEM of two experiments (n = 2–10; lower panel). **(F):** Confocal microscopy images of oval cells and TβT-OC. Representative images out of 2–3 experiments are shown. Scale bar: 20 µm. **(G):** *Hnf4alfa*, *Hnf1beta*, *GGT*, and *AFP* mRNA levels in oval cells and TβT-OC by quantitative reverse transcriptase-polymerase chain reaction. Data are mean ± SEM of 4–7 experiments (n = 3–18). In all cases, data were compared with the untreated group; *, $p < .05$; **, $p < .01$; ***, $p < .005$. At least three different TβT-OC lines were used in all analyses.

cells was confirmed by immunofluorescence staining of liver sections with anti-GFP antibody and PCR detection of the floxed allele in genomic DNA isolated from liver homogenate. Interestingly, GFP-positive cells are more abundant and form larger cell clusters in livers from mice transplanted with TβT-OC when compared with those transplanted with OC (Fig. 4B, 4C), suggesting a better engraftment or enhanced cell survival and/or proliferation upon engraftment. The following biochemical analysis of mouse serum revealed a significant improvement of liver function in mice transplanted with TβT-OC as compared with mice injected with parental cells or vehicle (PBS) only (Fig. 4D), as measured by reduced levels of alanine aminotransferase and aspartate aminotransferase induced by CCl_4 treatment. Likewise, transplantation of TβT-OC markedly diminished the extent of fibrosis and liver injury, with a clear reduction in collagen deposition, steatosis, and hepatocyte degeneration (Fig. 4E, 4F and Supporting Information S6). These results suggest that treatment with TGF-β confers oval cells unique properties that result in an attenuation of liver damage upon transplantation.

Lack of c-Met Tyrosine Kinase Activity Impedes Cell Expansion after Prolonged EMT by Inducing Replicative Senescence

Previous work from our laboratory showed a specific functional interaction between the HGF/c-Met axis and TGF-β pathway in oval cells [32, 33]. Here, we asked whether c-Met signaling could regulate the EMT response triggered by TGF-β. Using oval cells harboring, a genetically inactivated c-Met tyrosine kinase ($Met^{-/-}$) [32], we found that $Met^{-/-}$ oval cells undergo acute EMT upon TGF-β treatment in a same manner as their normal counterparts, $Met^{flx/flx}$ oval cells. Typical EMT features, including expression of EMT-inducing TFs, loss of E-cadherin and increased expression of mesenchymal markers (Supporting Information S7), were observed in both cell types, indicating that c-Met kinase activity does not interfere with acute induction of EMT by TGF-β in oval cells.

However, long-term expansion of $Met^{-/-}$ oval cells post-EMT was impaired due to cell inability to proliferate in culture. Early on during a subculture in the continuous presence of TGF-β, $Met^{-/-}$ oval cells suffered profound morphological changes and acquired a

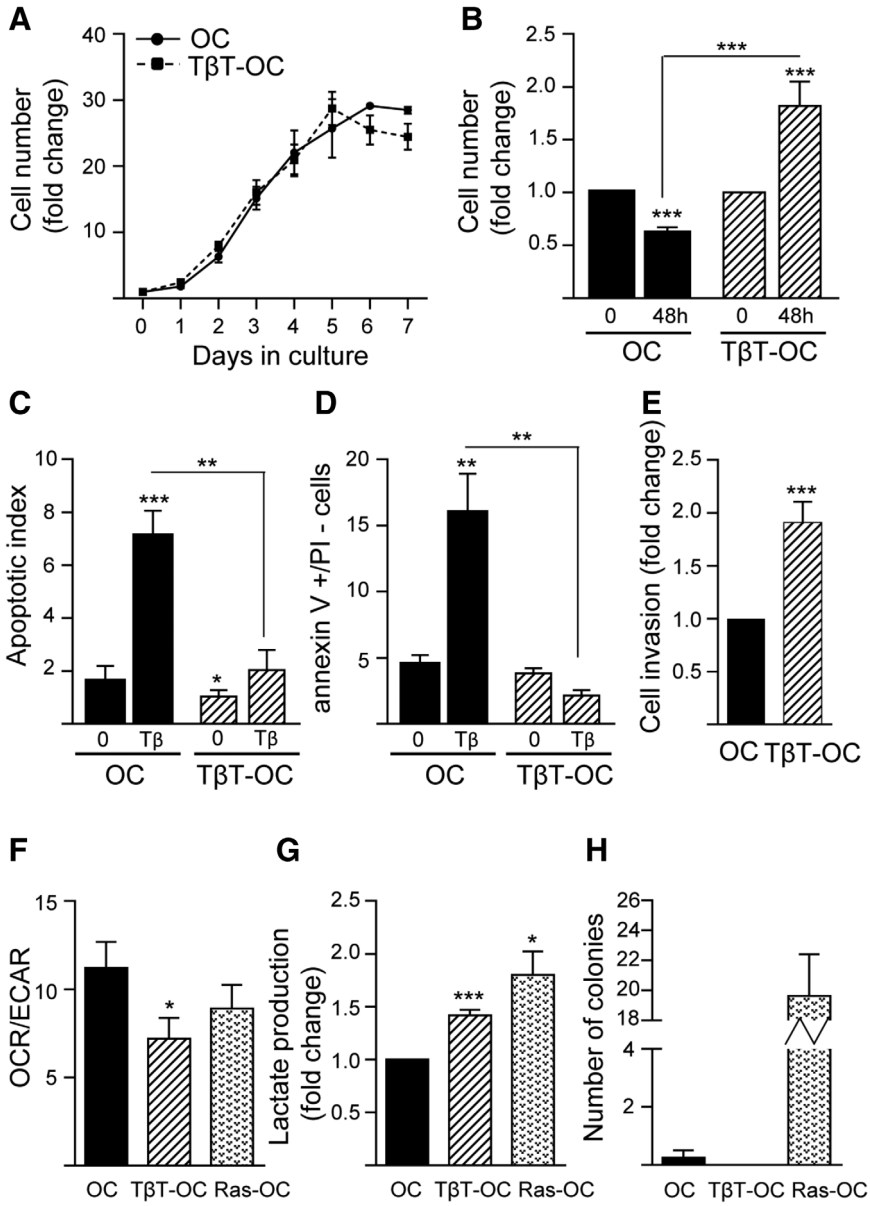

Figure 3. Changes in functional properties of oval cells after chronic treatment with transforming growth factor-β (TGF-β). **(A):** Oval cells and TβT-OC were cultured in 10% fetal bovine serum medium and counted. Data are expressed relative to time 0 and are mean ± SEM of 2–7 experiments performed in triplicate. **(B):** Oval cells and TβT-OC were cultured in serum-free medium for 48 hours and counted. Data are expressed relative to time 0 and are mean ± SEM of 14 experiments performed in triplicate. **(C, D):** Oval cells and TβT-OC were treated with TGF-β (1 ng/ml) for 24 hours in serum-free medium. (C): Quantification of apoptotic nuclei. Data are mean ± SEM of four experiments performed in triplicate. (D): Percentage of annexin V positive/PI negative cells analyzed by flow cytometry. Data are mean ± SEM (n = 6). **(E):** Cell invasion assay in matrigel-coated transwells. Data are mean ± SEM of nine experiments performed in triplicate. **(F):** OCR and extracellular acidification rate (ECAR) in oval cells, TβT-OC, and Ras-oval cells cultured in 25 mM glucose medium. Ratios OCR/ECAR were calculated. Data are mean ± SEM (n = 8). **(G):** Lactate production in oval cells, TβT-OC, and Ras-OC cultured in 25 mM glucose medium. Data are mean ± SEM of two independent experiments performed in triplicate. **(H):** Oval cells, TβT-oval cells, and Ras-oval cells were plated in soft agar and colonies were counted after 2 weeks. Data are mean ± SEM (n = 4). Data were compared with oval cell or untreated group or as indicated; *, $p < .05$; **, $p < .01$; ***, $p < .005$. At least three different TβT-OC lines were used.

senescent cell-like appearance (Fig. 5A) as judged by a SA-β Gal staining (Fig. 5B). Furthermore, the expression of the cyclin-dependent kinase inhibitors p15 and p19 was significantly higher in $Met^{-/-}$ oval cells as compared with $Met^{flx/flx}$ oval cells after subculture, which seems consistent with the irreversible growth arrest observed in $Met^{-/-}$ oval cells (Fig. 5C). These data suggested a critical role for c-Met in avoiding growth arrest after the EMT induced by TGF-β. To confirm our hypothesis, we run a comparative analysis of HGF mRNA expression and tyrosine phosphorylation of c-Met in oval cells and TβT-OC since we had described that oval cells present an autocrine signaling via HGF/c-Met that protect them from apoptosis [32]. Data confirmed that autocrine HGF/c-Met signaling remained operative after EMT (Fig. 5D and Supporting Information S8A). To further clarify the role of c-Met signaling in oval cell expansion and properties post-EMT, we used a c-Met tyrosine kinase activity inhibitor, PHA665752. PHA665752 completely abolished

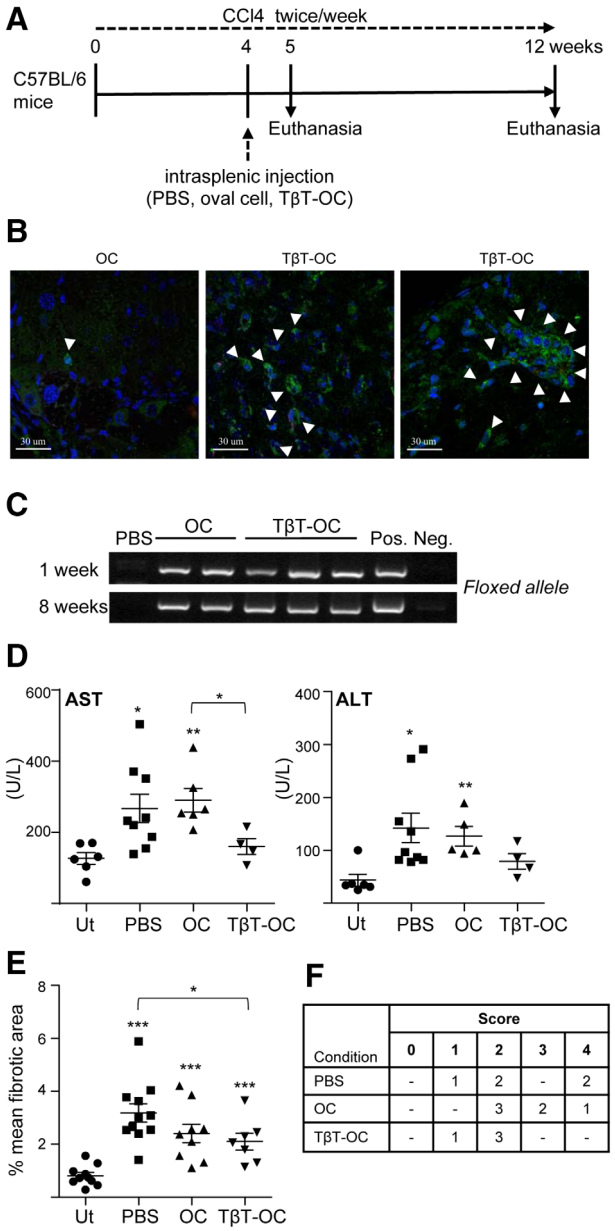

Figure 4. Transplantation of oval cells and TβT-OC into a damaged liver. **(A):** Scheme of CCl_4-induced liver fibrosis and cell transplantation assay. **(B):** Immunofluorescence staining was performed using a specific anti-GFP antibody in liver sections (1 week after transplantation). Representative images taken by confocal microscopy are shown. Arrowheads indicate GFP-positive cells corresponding to engrafted OC-GFP and TβT-OC-GFP. Scale bar: 30 μm. **(C):** Polymerase chain reaction genotyping to demonstrate the presence of the floxed allele in liver tissue samples from mice transplanted with OC, TβT-OC, or phosphate-buffered saline (PBS; as control) 1 and 8 weeks after transplantation. DNA from cultured oval cells and water were used as positive (Pos.) and negative (Neg.) control samples, respectively. **(D):** Analysis of aspartate aminotransferase and alanine aminotransferase serum levels in untreated (UT) mice and CCl_4-treated mice 8 weeks after transplantation of OC-GFP, TβT-OC-GFP, or PBS. Data are mean ± SEM of 4–9 animals per group. **(E):** Total area and fibrotic area (Sirius red-stained area) were measured in 10 regions per section using 4–6 animals per group (8 weeks post-transplant). Data are expressed as %mean of fibrotic area. **(F):** Histopathological assessment of liver damage (8 weeks post-transplant) in each experimental condition (n = 4–6) is indicated. Data were compared with UT or as indicated; *, $p < .05$; **, $p < .01$; ***, $p < .005$.

the HGF-induced c-Met phosphorylation and activation of its downstream target AKT (Supporting Information S8B). Importantly, pharmacological inhibition of c-Met signaling inhibited the intrinsic growth capacity exhibited by TβT-OC (Fig. 5E), which serves as additional proof of the existence of an autocrine signaling through HGF/c-Met which sustains their growth. The fact that cell number under PHA665752 treatment decreases below the baseline (zero time) suggests that c-Met inhibition affects also cell survival. Indeed, PHA665752 increased TβT-OC apoptotic index under serum withdrawal (Fig. 5F). Additionally, a moderate but significant decrease in cell invasive capacity was seen under PHA665752 treatment (Supporting Information S8C), which also shifted the balance toward mesenchymal cell traits (Fig. 5G). These results indicate that autocrine signaling via HGF/c-Met critically contributes to the phenotypical and functional properties acquired by oval cells after EMT.

However, the molecular mechanisms behind cellular senescence in $Met^{-/-}$ oval cells post-EMT were still unclear. Given that cellular senescence is strongly associated with oxidative stress and ROS production [43, 44], and our earlier data showed that TGF-β induces oxidative stress in oval cells [33], we hypothesized that oxidative stress might be the driving force of the senescence response characteristic for $Met^{-/-}$ oval cells undergoing EMT. In the early stages of chronic treatment with TGF-β, $Met^{-/-}$ oval cells displayed higher levels of ROS than $Met^{flx/flx}$ oval cells (Fig. 6A, 6B) and a stronger upregulation of Nox4 mRNA levels, a NADPH oxidase involved in TGF-β-induced ROS production [33, 45] (Fig. 6C and Supporting Information S4B, S4C). These data suggest that the senescence and growth arrest observed in $Met^{-/-}$ oval cells could be a consequence of an uncontrolled oxidative process. Interestingly, one of the key proteins that have been linked to abrogation of cellular senescence programs is Twist [46], which has been also described as an antioxidant factor [47]. This prompted us to check Twist levels in our cells. Twist was upregulated in TβT-OC (Supporting Information S9A). Besides, $Met^{-/-}$ oval cells expressed lower levels of Twist than $Met^{flx/flx}$ oval cells (Supporting Information S9B), and accordingly, HGF treatment in $Met^{flx/flx}$ oval cells resulted in Twist mRNA and protein levels upregulation, an effect that was abolished in the presence of the c-Met inhibitor (Fig. 6D, 6E). Additionally, we transiently knocked-down Twist in oval cells using siRNA, and then treated cells with TGF-β. A 70% reduction of Twist levels (Fig. 6F) led to significantly increased Nox4 levels after treatment with TGF-β as compared with cells transfected with nontargeting siRNA. Furthermore, p15 and p19 were strongly upregulated suggesting that Twist silencing results in an activation of senescence process (Fig. 6G).

Discussion

Plasticity of HPCs and their importance for liver homeostasis and regeneration are well known. However, more recent findings of the profibrogenic role and the potential of HPCs to become tumor initiating cells [2] are raising concerns regarding their real therapeutic utility. The key question is whether it is possible to modulate the HPCs fate to improve outcome of liver regeneration. Here, we provide novel evidence that the coordinated action of TGF-β and HGF may indeed enhance the regenerative potential of HPCs by promoting their beneficial traits.

Expression of mesenchymal markers found in rodent and human HPCs may suggest that they undergo EMT [48, 49].

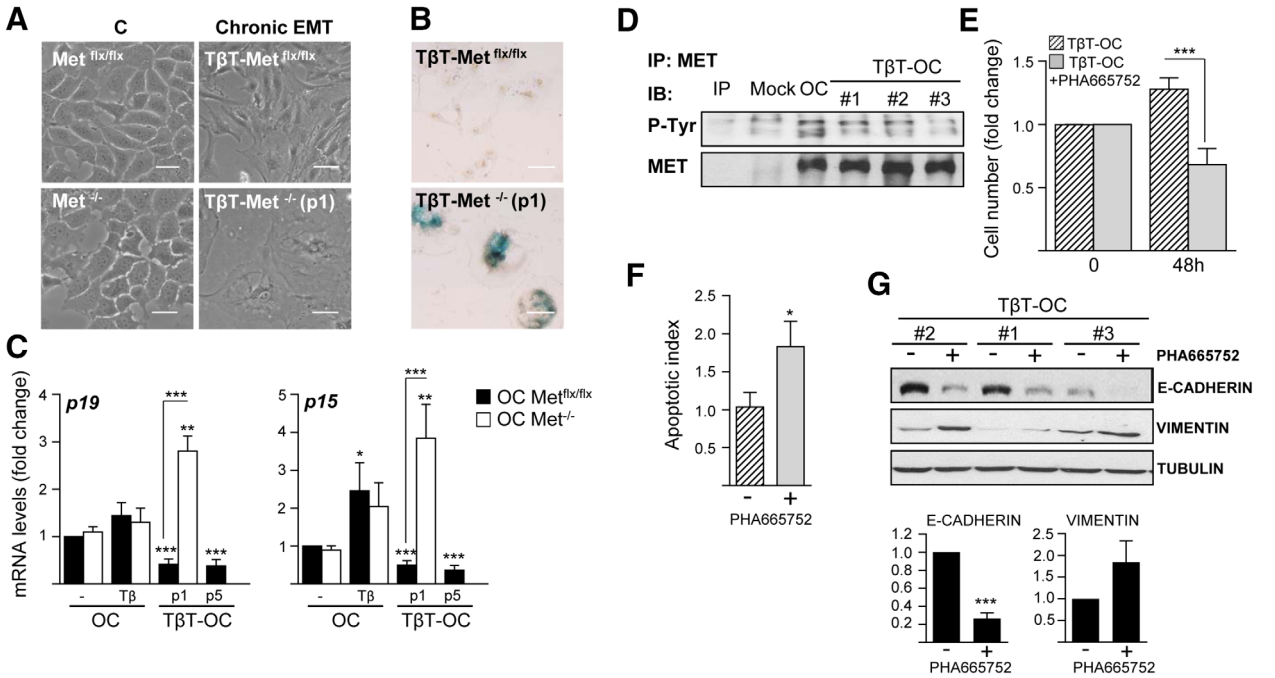

Figure 5. Lack of c-Met tyrosine kinase activity in oval cells leads to senescence after chronic treatment with transforming growth factor-β (TGF-β). **(A, B):** $Met^{fix/fix}$ and $Met^{-/-}$ oval cells were chronically treated with TGF-β (0.5 ng/ml). (A): Phase-contrast microscopy images of cell cultures. Scale bar: 50 μm. (B): Representative images after staining for SA-β-gal. Scale bar: 50 μm. **(C):** *p19* and *p15* mRNA levels in $Met^{fix/fix}$ and $Met^{-/-}$ oval cells untreated, acutely, or chronically treated with TGF-β at different passages (p1, p5) were determined by quantitative reverse transcriptase-polymerase chain reaction. Data are mean ± SEM (n = 3–8). **(D):** Whole protein extracts from oval cells and TβT-OC were used for Met immunoprecipitation. Phosphorylation was detected by immunoblotting with anti-P-tyrosine antibody. Western blot for Met was used as a loading control. A representative experiment (n = 4) using three different TβT-OC (designated #1, #2, and #3) is shown. **(E–G):** TβT-OC were treated with Met inhibitor PHA665752 (5 μM) for 2 weeks. (E): Cells were serum starved for 2 days and counted. Data are expressed relative to time 0 and are mean ± SEM of nine independent experiments performed in triplicate. (F): Quantification of apoptotic nuclei. Data are mean ± SEM of six experiments performed in triplicate. (G): Western blot analysis for E-cadherin and vimentin. One representative experiment using three different TβT-OC (designated #1, #2, and #3) is shown (upper panel). Optical density values are mean ± SEM (n = 6–9, lower panel). Data were compared with untreated group or as indicated; *, $p < .05$; **, $p < .01$; ***, $p < .005$. At least three different TβT-OC lines were used.

Consistent with this idea, several groups have reported that TGF-β induces EMT in rat HPCs in vitro which confers the characteristics of HSC and/or portal fibroblasts thereby contributing to fibrosis/cirrhosis progression [20, 50, 51] and to conversion into tumor initiating cells [52]. Other authors have proposed that HPCs could be derived from activated HSC through mesenchymal–epithelial transition (MET) [51]. Therefore, it seems that EMT–MET could play a role in regulation of HPCs function, although the overall situation is far from clear. Our results that both acute and chronic treatment with TGF-β induces EMT in mouse HPC (Fig. 1) agree with former in vitro evidence [20]. However, the coexpression of E-cadherin with mesenchymal markers N-cadherin and vimentin in chronically TGF-β-treated cells led us to propose that TGF-β triggers a partial rather than a full EMT. This strengthens the recent idea of EMT as a broad spectrum of transitional states [15], and is in line with the finding of partial EMT states in cultured HPCs, maintained at least in part by autocrine TGF-β and activin A/Smad signaling [53]. Further evidence supporting the intermediate EMT phenotype of TβT-OC is based on the coexpression of albumin and CK19 levels (Fig. 2), marker proteins of liver epithelial cells, together with CD44, a mesenchymal marker proven to be essential for TGF-β-induced EMT in HCC cells [38, 54, 55].

More striking are the data that EMT in oval cells did not result in enhancement of stem cell properties. Instead, we found a downregulation of epithelial stem cell-related markers Epcam and CD133 in TβT-OC and a decrease in clonal growth capacity (Fig. 2). Based on the expression pattern of biliary epithelial cell and hepatocyte markers, chronic treatment with TGF-β seemed to push oval cells further along the hepatic lineage. These results would argue against the link between the EMT and stemness described in other systems [37]. The convergence between these two processes might not always occur. In this sense, we earlier demonstrated that TGF-β besides inducing EMT also promotes a more differentiated phenotype in hepatocytes, particularly in the presence of HGF or EGF, resulting in a mixed phenotype in which liver specific genes and epithelial markers coexpressed with mesenchymal markers genes [56–59]. Likewise, HPCs from human fetal liver display a phenotype consistent with mesenchymal–epithelial transitional cells [60]. Furthermore, recent findings show that a sequential EMT–MET process drives differentiation of human embryonic stem cells toward hepatocytes, and that TGF-β and SNAI1 induction play a key role not only in EMT but also in definitive endoderm induction [61]. It seems that hepatocytic differentiation is tightly associated with EMT-MET phenotypic transitions, and that cooperation between TGF-β and growth factors could be critical in this process.

Our data highlight an essential role for HGF/c-Met pathway in the regulation of the extent of the TGF-β-induced EMT in oval cells since inhibition of c-Met in TβT-OC leads to a stronger mesenchymal phenotype (Fig. 5G). It is worth mentioning that although HGF/c-Met signaling drives EMT in some cell types, we

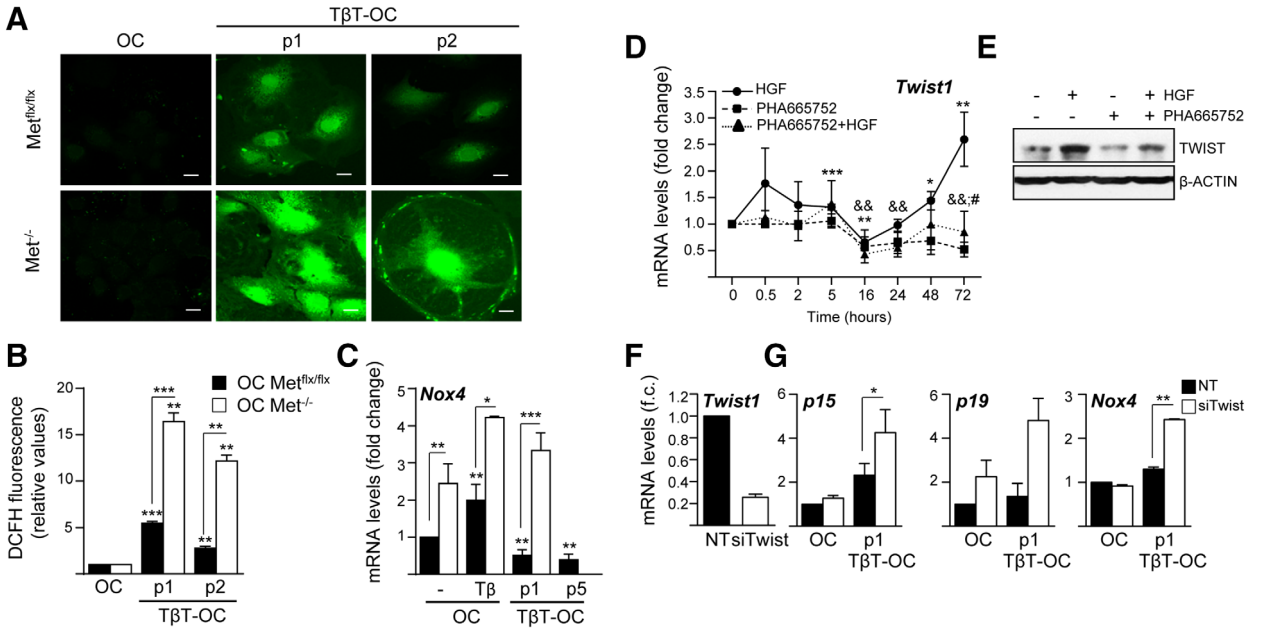

Figure 6. Epithelial–mesenchymal transition (EMT)-induced senescence in Met deficient oval cells is associated with enhanced oxidative stress and decreased twist expression. **(A, B):** $Met^{flx/flx}$, $Met^{-/-}$ oval cells, and TβT-OC at different passages were incubated with DCFH-DA (5 μM) for 30 minutes. (A): Confocal microscopy images from one experiment (n = 2). Scale bar: 20 μm. (B): DCFH-DA fluorescence intensity measured by flow cytometry. Data are mean ± SD (n = 3) from one representative experiment. **(C):** *Nox4* mRNA levels in $Met^{flx/flx}$ and $Met^{-/-}$ oval cells acutely or chronically treated with transforming growth factor-β (TGF-β; TβT-OC) at different passages were determined by quantitative reverse transcriptase-polymerase chain reaction (RT-qPCR). Data are mean ± SEM (n = 3–6). (B, C): Data were compared with untreated group or as indicated; *, $p < .05$; **, $p < .01$; ***, $p < .005$. **(D):** Cells were treated with hepatocyte growth factor (HGF; 40 ng/ml) ± PHA665752 (5 μM) and *Twist1* mRNA were determined by RT-qPCR. Data are expressed relative to untreated oval cells and are mean ± SEM (n = 2–6). Data were compared among them: untreated versus HGF; *, $p < .05$; **, $p < .01$; ***, $p < .005$; untreated versus PHA665752; #, $p < .05$; untreated versus PHA665752 + HGF; &&, $p < .01$. **(E):** Twist protein levels in oval cells treated with HGF (40 ng/ml) ± PHA665752 (5 μM) for 48 hours. One representative experiment (n = 3) is shown. **(F, G):** Oval cells were transfected with nontargeting negative control siRNA (NT) or Twist1 targeting siRNA (siTwist1). (F): *Twist1* mRNA levels determined by RT-qPCR. (G): *p15*, *p19*, and *Nox4* mRNA levels in NT and siTwist oval cells and TβT-OC at passage 1 (p1) were determined by RT-qPCR. Data are mean ± SEM (n = 2). Data were compared as indicated; *, $p < .05$; **, $p < .01$. Abbreviation: fc, fold change.

have proved that it is not the case in oval cells despite enhancing cell migration/invasion [62]. Here, we uncover a key contribution of the autocrine HGF/c-Met signaling in oval cells to counterbalance the TGF-β-induced EMT and to maintain and/or promote their epithelial properties. These results provide additional evidence of the HPC plasticity and importance of dynamic phenotypic transitional states of liver cells during liver injury, while pointing to an important functional cooperation between the TGF-β and HGF signaling pathways in its regulation.

The phenotypic changes provoked by EMT in oval cells in vitro are associated with growth, survival, migratory/invasive, and metabolic advantages (Fig. 3). Of note, EMT and its intermediate states have been recently identified as crucial drivers of organ fibrosis and tumor progression [15]. However, we found that upon transplantation, TβT-OC were able to significantly decrease the degree of liver fibrosis induced by CCl_4 and consequently improve liver functionality (Fig. 4). Altogether, these results raise two important issues. First, they serve as a proof of concept for the ability of oval cells to ameliorate liver fibrosis. Second, they demonstrate for the first time that EMT-induced traits can improve and/or accelerate the regenerative potential of oval cells facilitating the restoration of liver function upon injury.

The improved functional properties seen in TβT-OC are not solely due to the EMT-driven changes but to the contribution of the c-Met/HGF-triggered pathway. Using pharmacological inhibition of c-Met kinase activity, we demonstrate that an HGF/c-Met autocrine signaling in oval cells [32] is essential for the functional advantages acquired after EMT, including growth, survival, and invasion capacities (Fig. 5 and Supporting Information S8C).

Our work also reveals an interesting inverse correlation between c-Met signaling and senescence induction during EMT. Previously, it has been shown that loss/suppression of Zeb1 or Twist triggered a premature senescence program [63, 64] linking senescence and EMT. More specifically, Twist 1 and 2 blocked the suppressor proteins pRb and p53, cooperating with oncoproteins such as H-Ras to induce a full EMT and cell invasion [65]. Our data support the concept that overcoming senescence is a critical step for cell expansion upon EMT induction, highlighting a role for HGF/c-Met in this process. Thus, results suggest an interesting scenario where c-Met signaling via Twist induction would control TGF-β-induced oxidative stress, which in turn may overcome cell senescence and allow cell survival and expansion. It is well-known that excessive ROS production causes oxidative stress and subsequently induces cell senescence or cell death [66]. The powerful antioxidant activity of c-Met in liver cells and particularly oval cells supports previous data [33, 67]. Less known is the antioxidant activity of Twist proteins, which has been linked to their antiapoptotic effects [47]. Our data provide the first evidence suggesting a role for Twist in the HGF/c-Met antioxidant activity. However, these results appear to contradict the established idea of Twist as an EMT-inducing TF since HGF/c-Met signaling in TβT-OC help maintain epithelial properties. In this regard, studies in a

model of bone metastatic and parental breast carcinoma cells revealed that induction of a MET process by HGF involves E-cadherin upregulation via activation of a Twist program. Notably, a coordinated action of HGF and TGF-β is also reported in this context [68]. Taken together, these data suggest that the dynamic EMT-MET switch is complex and involves multitude of regulatory interactions in which HGF and TGF-β appear to play central roles.

Conclusion

Our work provides evidence that the balance between HGF and TGF-β signaling pathways might be critical for oval cell fate and outcome of liver regeneration. We propose a scenario where HGF/c-Met signaling restrains TGF-β effects. This allows maintaining a controlled oxidative stress and apoptotic response thereby promoting the expansion of oval cells and overall improving the regenerative potential of oval cells. The potential therapeutic implications of these findings warrant further investigation.

Acknowledgments

This work was supported by a Marie Curie Action FP7-2012 (grant #PITN-GA-2012-316549; IT-LIVER); Ministry of Science, Innovation and Universities, Spain (grant #SAF2015-69145-R); and General Direction of Universities and Research of the Autonomous Community of Madrid, Spain (grant #S2010/BMD-2402, MITOLAB consortium). Financial sources had no involvement in study design or in data analysis. L.A. was recipient of a predoctoral contract from UCM. M.G.-A., A.M.-P., and N.L. were recipients from research-training contracts from grant #S2010/BMD-2402 and SAF2006-12025 (Ministry of Education and Science) and SAF2015-69145-R, respectively. A.A. was recipient of a Marie Curie ESR contract from IT-LIVER. We thank Dr. G. Velasco for kindly providing CD133 antibody and Dr. M. Fernández for helpful discussions. S.S.T. is currently affiliated with the Laboratory of Human Carcinogenesis, Center for Cancer Research, National Cancer Institute, National Institutes of Health, Bethesda, MD.

Author Contributions

L.A., A.M.-P., C.R., J.S., E.R.: collection and/or assembly of data, data analysis and interpretation, final approval of manuscript; M.G.-A., M.G.-B., N.L., A.A., M.d.O.L., P.B.: collection and/or assembly of data, final approval of manuscript; W.M., J.I.C.: provision of study material or patients, final approval of manuscript; V.M.F., S.S.T., I.F.: data analysis and interpretation, final approval of manuscript; J.-C.S.: conception and design, final approval of manuscript; B.H., A.S.: conception and design, data analysis and interpretation, manuscript writing, final approval of manuscript.

Disclosure of Potential Conflicts of Interest

The authors indicated no potential conflicts of interest.

Data Availability Statement

The data that support the findings of this study are available from the corresponding author upon reasonable request.

References

1 Itoh T, Miyajima A. Liver regeneration by stem/progenitor cells. Hepatology 2014; 59:1617–1626.
2 Kohn-Gaone J, Gogoi-Tiwari J, Ramm GA et al. The role of liver progenitor cells during liver regeneration, fibrogenesis, and carcinogenesis. Am J Physiol Gastrointest Liver Physiol 2016;310:G143–G154.
3 Clouston AD, Powell EE, Walsh MJ et al. Fibrosis correlates with a ductular reaction in hepatitis C: Roles of impaired replication, progenitor cells and steatosis. Hepatology 2005;41:809–818.
4 Kuramitsu K, Sverdlov DY, Liu SB et al. Failure of fibrotic liver regeneration in mice is linked to a severe fibrogenic response driven by hepatic progenitor cell activation. Am J Pathol 2013;183:182–194.
5 Giannelli G, Mikulits W, Dooley S et al. The rationale for targeting TGF-beta in chronic liver diseases. Eur J Clin Invest 2016;46:349–361.
6 Dooley S, ten Dijke P. TGF-beta in progression of liver disease. Cell Tissue Res 2012; 347:245–256.
7 Puche JE, Saiman Y, Friedman SL. Hepatic stellate cells and liver fibrosis. Compr Physiol 2013;3:1473–1492.
8 Brenner DA. Molecular pathogenesis of liver fibrosis. Trans Am Clin Climatol Assoc 2009;120:361–368.
9 Herrera B, Alvarez AM, Sanchez A et al. Reactive oxygen species (ROS) mediates the mitochondrial-dependent apoptosis induced by transforming growth factor (beta) in fetal hepatocytes. FASEB J 2001;15:741–751.
10 Sanchez A, Alvarez AM, Benito M et al. Apoptosis induced by transforming growth factor-beta in fetal hepatocyte primary cultures: Involvement of reactive oxygen intermediates. J Biol Chem 1996;271:7416–7422.
11 Richter K, Kietzmann T. Reactive oxygen species and fibrosis: Further evidence of a significant liaison. Cell Tissue Res 2016;365: 591–605.
12 Czaja AJ. Hepatic inflammation and progressive liver fibrosis in chronic liver disease. World J Gastroenterol 2014;20:2515–2532.
13 Gonzalez DM, Medici D. Signaling mechanisms of the epithelial–mesenchymal transition. Sci Signal 2014;7:re8.
14 Valdes F, Alvarez AM, Locascio A et al. The epithelial mesenchymal transition confers resistance to the apoptotic effects of transforming growth factor beta in fetal rat hepatocytes. Mol Cancer Res 2002;1:68–78.
15 Nieto MA, Huang RY, Jackson RA et al. Emt: 2016. Cell 2016;166:21–45.
16 Chu AS, Diaz R, Hui JJ et al. Lineage tracing demonstrates no evidence of cholangiocyte epithelial-to-mesenchymal transition in murine models of hepatic fibrosis. Hepatology 2011; 53:1685–1695.
17 Dooley S, Hamzavi J, Ciuclan L et al. Hepatocyte-specific Smad7 expression attenuates TGF-beta-mediated fibrogenesis and protects against liver damage. Gastroenterology 2008;135:642–659.
18 Taura K, Miura K, Iwaisako K et al. Hepatocytes do not undergo epithelial–mesenchymal transition in liver fibrosis in mice. Hepatology 2010;51:1027–1036.
19 Wells RG. The epithelial-to-mesenchymal transition in liver fibrosis: Here today, gone tomorrow? Hepatology 2010;51:737–740.
20 Wang P, Liu T, Cong M et al. Expression of extracellular matrix genes in cultured hepatic oval cells: An origin of hepatic stellate cells through transforming growth factor beta? Liver Int 2009;29:575–584.
21 Wang P, Yang AT, Cong M et al. EGF suppresses the initiation and drives the reversion of TGF-beta1-induced transition in hepatic oval cells showing the plasticity of progenitor cells. J Cell Physiol 2015;230:2362–2370.
22 Nishino M, Iimuro Y, Ueki T et al. Hepatocyte growth factor improves survival after partial hepatectomy in cirrhotic rats suppressing apoptosis of hepatocytes. Surgery 2008;144: 374–384.
23 Jiang D, Jiang Z, Li Z et al. Suppression of the production of extracellular matrix and alpha-smooth muscle actin induced by transforming growth factor-beta1 in fibroblasts of the flexor tendon sheath by hepatocyte growth factor. Scand J Plast Reconstr Surg Hand Surg 2008;42: 169–173.
24 Li F, Sun JY, Wang JY et al. Effect of hepatocyte growth factor encapsulated in targeted

liposomes on liver cirrhosis. J Control Release 2008;131:77–82.
25 Inagaki Y, Higashi K, Kushida M et al. Hepatocyte growth factor suppresses profibrogenic signal transduction via nuclear export of Smad3 with galectin-7. Gastroenterology 2008;134:1180–1190.
26 Kanemura H, Iimuro Y, Takeuchi M et al. Hepatocyte growth factor gene transfer with naked plasmid DNA ameliorates dimethylnitrosamine-induced liver fibrosis in rats. Hepatol Res 2008;38:930–939.
27 Ueki T, Kaneda Y, Tsutsui H et al. Hepatocyte growth factor gene therapy of liver cirrhosis in rats. Nat Med 1999;5:226–230.
28 Xia JL, Dai C, Michalopoulos GK et al. Hepatocyte growth factor attenuates liver fibrosis induced by bile duct ligation. Am J Pathol 2006;168:1500–1512.
29 Huh CG, Factor VM, Sanchez A et al. Hepatocyte growth factor/c-met signaling pathway is required for efficient liver regeneration and repair. Proc Natl Acad Sci USA 2004;101:4477–4482.
30 Ishikawa T, Factor VM, Marquardt JU et al. Hepatocyte growth factor/c-met signaling is required for stem-cell-mediated liver regeneration in mice. Hepatology 2012;55:1215–1226.
31 Marquardt JU, Seo D, Gomez-Quiroz LE et al. Loss of c-Met accelerates development of liver fibrosis in response to CCl(4) exposure through deregulation of multiple molecular pathways. Biochim Biophys Acta 2012;1822:942–951.
32 del Castillo G, Factor VM, Fernandez M et al. Deletion of the Met tyrosine kinase in liver progenitor oval cells increases sensitivity to apoptosis in vitro. Am J Pathol 2008;172:1238–1247.
33 Martinez-Palacian A, del Castillo G, Suarez-Causado A et al. Mouse hepatic oval cells require Met-dependent PI3K to impair TGF-beta-induced oxidative stress and apoptosis. PLoS One 2013;8:e53108.
34 Awan SJ, Baig MT, Yaqub F et al. In vitro differentiated hepatic oval-like cells enhance hepatic regeneration in CCl4-induced hepatic injury. Cell Biol Int 2017;41:51–61.
35 Liu LX, Lee NP, Chan VW et al. Targeting cadherin-17 inactivates Wnt signaling and inhibits tumor growth in liver carcinoma. Hepatology 2009;50:1453–1463.
36 Polette M, Mestdagt M, Bindels S et al. Beta-catenin and ZO-1: Shuttle molecules involved in tumor invasion-associated epithelial–mesenchymal transition processes. Cells Tissues Organs 2007;185:61–65.
37 Fabregat I, Malfettone A, Soukupova J. New insights into the crossroads between EMT and stemness in the context of cancer. J Clin Med 2016;5:pii: E37 (1–12).
38 Malfettone A, Soukupova J, Bertran E et al. Transforming growth factor-beta-induced plasticity causes a migratory stemness phenotype in hepatocellular carcinoma. Cancer Lett 2017;392:39–50.
39 Chen J, Chen L, Zern MA et al. The diversity and plasticity of adult hepatic progenitor cells and their niche. Liver Int 2017;37:1260–1271.
40 Watt AJ, Garrison WD, Duncan SA. HNF4: A central regulator of hepatocyte differentiation and function. Hepatology 2003;37:1249–1253.
41 Brabletz T, Kalluri R, Nieto MA et al. EMT in cancer. Nat Rev Cancer 2018;18:128–134.
42 Kim DH, Xing T, Yang Z et al. Epithelial mesenchymal transition in embryonic development, tissue repair and cancer: A comprehensive overview. J Clin Med 2017;7:pii: E1 (1–25).
43 Chandrasekaran A, Idelchik M, Melendez JA. Redox control of senescence and age-related disease. Redox Biol 2017;11:91–102.
44 Hernandez-Segura A, Nehme J, Demaria M. Hallmarks of cellular senescence. Trends Cell Biol 2018;28:436–453.
45 Carmona-Cuenca I, Roncero C, Sancho P et al. Upregulation of the NADPH oxidase NOX4 by TGF-beta in hepatocytes is required for its pro-apoptotic activity. J Hepatol 2008; 49:965–976.
46 Zhao Z, Rahman MA, Chen ZG et al. Multiple biological functions of Twist1 in various cancers. Oncotarget 2017;8:20380–20393.
47 Floc'h N, Kolodziejski J, Akkari L et al. Modulation of oxidative stress by twist oncoproteins. PLoS One 2013;8:e72490.
48 Yovchev MI, Grozdanov PN, Zhou H et al. Identification of adult hepatic progenitor cells capable of repopulating injured rat liver. Hepatology 2008;47:636–647.
49 Syn WK, Jung Y, Omenetti A et al. Hedgehog-mediated epithelial-to-mesenchymal transition and fibrogenic repair in nonalcoholic fatty liver disease. Gastroenterology 2009;137:1478. e1478–1488.e1478.
50 Chen J, Zhang X, Xu Y et al. Hepatic progenitor cells contribute to the progression of 2-acetylaminofluorene/carbon tetrachloride-induced cirrhosis via the non-canonical Wnt pathway. PLoS One 2015;10:e0130310.
51 Deng H, Wang HF, Gao YB et al. Hepatic progenitor cell represents a transitioning cell population between liver epithelium and stroma. Med Hypotheses 2011;76:809–812.
52 Wu K, Ding J, Chen C et al. Hepatic transforming growth factor beta gives rise to tumor-initiating cells and promotes liver cancer development. Hepatology 2012;56:2255–2267.
53 Wu Y, Ding ZY, Jin GN et al. Autocrine transforming growth factor-beta/activin A-Smad signaling induces hepatic progenitor cells undergoing partial epithelial–mesenchymal transition states. Biochimie 2018;148:87–98.
54 Gao Y, Ruan B, Liu W et al. Knockdown of CD44 inhibits the invasion and metastasis of hepatocellular carcinoma both in vitro and in vivo by reversing epithelial–mesenchymal transition. Oncotarget 2015;6:7828–7837.
55 Mima K, Okabe H, Ishimoto T et al. CD44s regulates the TGF-beta-mediated mesenchymal phenotype and is associated with poor prognosis in patients with hepatocellular carcinoma. Cancer Res 2012;72:3414–3423.
56 Pagan R, Martin I, Llobera M et al. Growth and differentiation factors inhibit the migratory phenotype of cultured neonatal rat hepatocytes induced by HGF/SF. Exp Cell Res 1997;235:170–179.
57 Pagan R, Sanchez A, Martin I et al. Effects of growth and differentiation factors on the epithelial–mesenchymal transition in cultured neonatal rat hepatocytes. J Hepatol 1999;31:895–904.
58 Sanchez A, Alvarez AM, Benito M et al. Transforming growth factor beta modulates growth and differentiation of fetal hepatocytes in primary culture. J Cell Physiol 1995; 165:398–405.
59 Sanchez A, Pagan R, Alvarez AM et al. Transforming growth factor-beta (TGF-beta) and EGF promote cord-like structures that indicate terminal differentiation of fetal hepatocytes in primary culture. Exp Cell Res 1998;242:27–37.
60 Dan YY, Riehle KJ, Lazaro C et al. Isolation of multipotent progenitor cells from human fetal liver capable of differentiating into liver and mesenchymal lineages. Proc Natl Acad Sci USA 2006;103:9912–9917.
61 Li Q, Hutchins AP, Chen Y et al. A sequential EMT-MET mechanism drives the differentiation of human embryonic stem cells towards hepatocytes. Nat Commun 2017;8:15166.
62 Suarez-Causado A, Caballero-Diaz D, Bertran E et al. HGF/c-Met signaling promotes liver progenitor cell migration and invasion by an epithelial-mesenchymal transition-independent, phosphatidyl inositol-3 kinase-dependent pathway in an in vitro model. Biochim Biophys Acta 2015;1853:2453–2463.
63 Brabletz S, Brabletz T. The ZEB/miR-200 feedback loop—A motor of cellular plasticity in development and cancer? EMBO Rep 2010; 11:670–677.
64 Burns TF, Dobromilskaya I, Murphy SC et al. Inhibition of TWIST1 leads to activation of oncogene-induced senescence in oncogene-driven non-small cell lung cancer. Mol Cancer Res 2013;11:329–338.
65 Ansieau S, Bastid J, Doreau A et al. Induction of EMT by twist proteins as a collateral effect of tumor-promoting inactivation of premature senescence. Cancer Cell 2008;14:79–89.
66 Wei W, Ji S. Cellular senescence: Molecular mechanisms and pathogenicity. J Cell Physiol 2018;233:9121–9135.
67 Gomez-Quiroz LE, Factor VM, Kaposi-Novak P et al. Hepatocyte-specific c-Met deletion disrupts redox homeostasis and sensitizes to Fas-mediated apoptosis. J Biol Chem 2008; 283:14581–14589.
68 Bendinelli P, Maroni P, Matteucci E et al. HGF and TGFbeta1 differently influenced Wwox regulatory function on Twist program for mesenchymal–epithelial transition in bone metastatic versus parental breast carcinoma cells. Mol Cancer 2015;14:112.


See www.StemCells.com for supporting information available online.